Single Electrons from Heavy Flavor Decays in p+p Collisions at $\sqrt{s} = 200$ GeV

S.S. Adler,[5] S. Afanasiev,[17] C. Aidala,[5] N.N. Ajitanand,[43] Y. Akiba,[20,38] J. Alexander,[43] R. Amirikas,[12] L. Aphecetche,[45] S.H. Aronson,[5] R. Averbeck,[44] T.C. Awes,[35] R. Azmoun,[44] V. Babintsev,[15] A. Baldisseri,[10] K.N. Barish,[6] P.D. Barnes,[27] B. Bassalleck,[33] S. Bathe,[30] S. Batsouli,[9] V. Baublis,[37] A. Bazilevsky,[39,15] S. Belikov,[16,15] Y. Berdnikov,[40] S. Bhagavatula,[16] J.G. Boissevain,[27] H. Borel,[10] S. Borenstein,[25] M.L. Brooks,[27] D.S. Brown,[34] N. Bruner,[33] D. Bucher,[30] H. Buesching,[30] V. Bumazhnov,[15] G. Bunce,[5,39] J.M. Burward-Hoy,[26,44] S. Butsyk,[44] X. Camard,[45] J.-S. Chai,[18] P. Chand,[4] W.C. Chang,[2] S. Chernichenko,[15] C.Y. Chi,[9] J. Chiba,[20] M. Chiu,[9] I.J. Choi,[52] J. Choi,[19] R.K. Choudhury,[4] T. Chujo,[5] V. Cianciolo,[35] Y. Cobigo,[10] B.A. Cole,[9] P. Constantin,[16] D. d'Enterria,[45] G. David,[5] H. Delagrange,[45] A. Denisov,[15] A. Deshpande,[39] E.J. Desmond,[5] A. Devismes,[44] O. Dietzsch,[41] O. Drapier,[25] A. Drees,[44] R. du Rietz,[29] A. Durum,[15] D. Dutta,[4] Y.V. Efremenko,[35] K. El Chenawi,[49] A. Enokizono,[14] H. En'yo,[38,39] S. Esumi,[48] L. Ewell,[5] D.E. Fields,[33,39] F. Fleuret,[25] S.L. Fokin,[23] B.D. Fox,[39] Z. Fraenkel,[51] J.E. Frantz,[9] A. Franz,[5] A.D. Frawley,[12] S.-Y. Fung,[6] S. Garpman,[29,*] T.K. Ghosh,[49] A. Glenn,[46] G. Gogiberidze,[46] M. Gonin,[25] J. Gosset,[10] Y. Goto,[39] R. Granier de Cassagnac,[25] N. Grau,[16] S.V. Greene,[49] M. Grosse Perdekamp,[39] W. Guryn,[5] H.-Å. Gustafsson,[29] T. Hachiya,[14] J.S. Haggerty,[5] H. Hamagaki,[8] A.G. Hansen,[27] E.P. Hartouni,[26] M. Harvey,[5] R. Hayano,[8] N. Hayashi,[38] X. He,[13] M. Heffner,[26] T.K. Hemmick,[44] J.M. Heuser,[44] M. Hibino,[50] J.C. Hill,[16] W. Holzmann,[43] K. Homma,[14] B. Hong,[22] A. Hoover,[34] T. Ichihara,[38,39] V.V. Ikonnikov,[23] K. Imai,[24,38] D. Isenhower,[1] M. Ishihara,[38] M. Issah,[43] A. Isupov,[17] B.V. Jacak,[44] W.Y. Jang,[22] Y. Jeong,[19] J. Jia,[44] O. Jinnouchi,[38] B.M. Johnson,[5] S.C. Johnson,[26] K.S. Joo,[31] D. Jouan,[36] S. Kametani,[8,50] N. Kamihara,[47,38] J.H. Kang,[52] S.S. Kapoor,[4] K. Katou,[50] S. Kelly,[9] B. Khachaturov,[51] A. Khanzadeev,[37] J. Kikuchi,[50] D.H. Kim,[31] D.J. Kim,[52] D.W. Kim,[19] E. Kim,[42] G.-B. Kim,[25] H.J. Kim,[52] E. Kistenev,[5] A. Kiyomichi,[48] K. Kiyoyama,[32] C. Klein-Boesing,[30] H. Kobayashi,[38,39] L. Kochenda,[37] V. Kochetkov,[15] D. Koehler,[33] T. Kohama,[14] M. Kopytine,[44] D. Kotchetkov,[6] A. Kozlov,[51] P.J. Kroon,[5] C.H. Kuberg,[1,27] K. Kurita,[39] Y. Kuroki,[48] M.J. Kweon,[22] Y. Kwon,[52] G.S. Kyle,[34] R. Lacey,[43] V. Ladygin,[17] J.G. Lajoie,[16] A. Lebedev,[16,23] S. Leckey,[44] D.M. Lee,[27] S. Lee,[19] M.J. Leitch,[27] X.H. Li,[6] H. Lim,[42] A. Litvinenko,[17] M.X. Liu,[27] Y. Liu,[36] C.F. Maguire,[49] Y.I. Makdisi,[5] A. Malakhov,[17] V.I. Manko,[23] Y. Mao,[7,38] G. Martinez,[45] M.D. Marx,[44] H. Masui,[48] F. Matathias,[44] T. Matsumoto,[8,50] P.L. McGaughey,[27] E. Melnikov,[15] F. Messer,[44] Y. Miake,[48] J. Milan,[43] T.E. Miller,[49] A. Milov,[44,51] S. Mioduszewski,[5] R.E. Mischke,[27] G.C. Mishra,[13] J.T. Mitchell,[5] A.K. Mohanty,[4] D.P. Morrison,[5] J.M. Moss,[27] F. Mühlbacher,[44] D. Mukhopadhyay,[51] M. Muniruzzaman,[6] J. Murata,[38,39] S. Nagamiya,[20] J.L. Nagle,[9] T. Nakamura,[14] B.K. Nandi,[6] M. Nara,[48] J. Newby,[46] P. Nilsson,[29] A.S. Nyanin,[23] J. Nystrand,[29] E. O'Brien,[5] C.A. Ogilvie,[16] H. Ohnishi,[5,38] I.D. Ojha,[49,3] K. Okada,[38] M. Ono,[48] V. Onuchin,[15] A. Oskarsson,[29] I. Otterlund,[29] K. Oyama,[8] K. Ozawa,[8] D. Pal,[51] A.P.T. Palounek,[27] V. Pantuev,[44] V. Papavassiliou,[34] J. Park,[42] A. Parmar,[33] S.F. Pate,[34] T. Peitzmann,[30] J.-C. Peng,[27] V. Peresedov,[17] C. Pinkenburg,[5] R.P. Pisani,[5] F. Plasil,[35] M.L. Purschke,[5] A.K. Purwar,[44] J. Rak,[16] I. Ravinovich,[51] K.F. Read,[35,46] M. Reuter,[44] K. Reygers,[30] V. Riabov,[37,40] Y. Riabov,[37] G. Roche,[28] A. Romana,[25] M. Rosati,[16] P. Rosnet,[28] S.S. Ryu,[52] M.E. Sadler,[1] N. Saito,[38,39] T. Sakaguchi,[8,50] M. Sakai,[32] S. Sakai,[48] V. Samsonov,[37] L. Sanfratello,[33] R. Santo,[30] H.D. Sato,[24,38] S. Sato,[5,48] S. Sawada,[20] Y. Schutz,[45] V. Semenov,[15] R. Seto,[6] M.R. Shaw,[1,27] T.K. Shea,[5] T.-A. Shibata,[47,38] K. Shigaki,[14,20] T. Shiina,[27] C.L. Silva,[41] D. Silvermyr,[27,29] K.S. Sim,[22] C.P. Singh,[3] V. Singh,[3] M. Sivertz,[5] A. Soldatov,[15] R.A. Soltz,[26] W.E. Sondheim,[27] S.P. Sorensen,[46] I.V. Sourikova,[5] F. Staley,[10] P.W. Stankus,[35] E. Stenlund,[29] M. Stepanov,[34] A. Ster,[21] S.P. Stoll,[5] T. Sugitate,[14] J.P. Sullivan,[27] E.M. Takagui,[41] A. Taketani,[38,39] M. Tamai,[50] K.H. Tanaka,[20] Y. Tanaka,[32] K. Tanida,[38] M.J. Tannenbaum,[5] P. Tarján,[11] J.D. Tepe,[1,27] T.L. Thomas,[33] J. Tojo,[24,38] H. Torii,[24,38] R.S. Towell,[1] I. Tserruya,[51] H. Tsuruoka,[48] S.K. Tuli,[3] H. Tydesjö,[29] N. Tyurin,[15] H.W. van Hecke,[27] J. Velkovska,[5,44] M. Velkovsky,[44] V. Veszprémi,[11] L. Villatte,[46] A.A. Vinogradov,[23] M.A. Volkov,[23] E. Vznuzdaev,[37] X.R. Wang,[13] Y. Watanabe,[38,39] S.N. White,[5] F.K. Wohn,[16] C.L. Woody,[5] W. Xie,[6] Y. Yang,[7] A. Yanovich,[15] S. Yokkaichi,[38,39] G.R. Young,[35] I.E. Yushmanov,[23] W.A. Zajc,[9,†] C. Zhang,[9] S. Zhou,[7] S.J. Zhou,[51] and L. Zolin[17]

(PHENIX Collaboration)

[1]Abilene Christian University, Abilene, TX 79699, USA
[2]Institute of Physics, Academia Sinica, Taipei 11529, Taiwan
[3]Department of Physics, Banaras Hindu University, Varanasi 221005, India
[4]Bhabha Atomic Research Centre, Bombay 400 085, India
[5]Brookhaven National Laboratory, Upton, NY 11973-5000, USA

[6]University of California - Riverside, Riverside, CA 92521, USA
[7]China Institute of Atomic Energy (CIAE), Beijing, People's Republic of China
[8]Center for Nuclear Study, Graduate School of Science, University of Tokyo, 7-3-1 Hongo, Bunkyo, Tokyo 113-0033, Japan
[9]Columbia University, New York, NY 10027 and Nevis Laboratories, Irvington, NY 10533, USA
[10]Dapnia, CEA Saclay, F-91191, Gif-sur-Yvette, France
[11]Debrecen University, H-4010 Debrecen, Egyetem tér 1, Hungary
[12]Florida State University, Tallahassee, FL 32306, USA
[13]Georgia State University, Atlanta, GA 30303, USA
[14]Hiroshima University, Kagamiyama, Higashi-Hiroshima 739-8526, Japan
[15]IHEP Protvino, State Research Center of Russian Federation, Institute for High Energy Physics, Protvino, 142281, Russia
[16]Iowa State University, Ames, IA 50011, USA
[17]Joint Institute for Nuclear Research, 141980 Dubna, Moscow Region, Russia
[18]KAERI, Cyclotron Application Laboratory, Seoul, South Korea
[19]Kangnung National University, Kangnung 210-702, South Korea
[20]KEK, High Energy Accelerator Research Organization, Tsukuba, Ibaraki 305-0801, Japan
[21]KFKI Research Institute for Particle and Nuclear Physics of the Hungarian Academy of Sciences (MTA KFKI RMKI), H-1525 Budapest 114, POBox 49, Budapest, Hungary
[22]Korea University, Seoul, 136-701, Korea
[23]Russian Research Center "Kurchatov Institute", Moscow, Russia
[24]Kyoto University, Kyoto 606-8502, Japan
[25]Laboratoire Leprince-Ringuet, Ecole Polytechnique, CNRS-IN2P3, Route de Saclay, F-91128, Palaiseau, France
[26]Lawrence Livermore National Laboratory, Livermore, CA 94550, USA
[27]Los Alamos National Laboratory, Los Alamos, NM 87545, USA
[28]LPC, Université Blaise Pascal, CNRS-IN2P3, Clermont-Fd, 63177 Aubiere Cedex, France
[29]Department of Physics, Lund University, Box 118, SE-221 00 Lund, Sweden
[30]Institut für Kernphysik, University of Muenster, D-48149 Muenster, Germany
[31]Myongji University, Yongin, Kyonggido 449-728, Korea
[32]Nagasaki Institute of Applied Science, Nagasaki-shi, Nagasaki 851-0193, Japan
[33]University of New Mexico, Albuquerque, NM 87131, USA
[34]New Mexico State University, Las Cruces, NM 88003, USA
[35]Oak Ridge National Laboratory, Oak Ridge, TN 37831, USA
[36]IPN-Orsay, Universite Paris Sud, CNRS-IN2P3, BP1, F-91406, Orsay, France
[37]PNPI, Petersburg Nuclear Physics Institute, Gatchina, Leningrad region, 188300, Russia
[38]RIKEN, The Institute of Physical and Chemical Research, Wako, Saitama 351-0198, Japan
[39]RIKEN BNL Research Center, Brookhaven National Laboratory, Upton, NY 11973-5000, USA
[40]Saint Petersburg State Polytechnic University, St. Petersburg, Russia
[41]Universidade de São Paulo, Instituto de Física, Caixa Postal 66318, São Paulo CEP05315-970, Brazil
[42]System Electronics Laboratory, Seoul National University, Seoul, South Korea
[43]Chemistry Department, Stony Brook University, SUNY, Stony Brook, NY 11794-3400, USA
[44]Department of Physics and Astronomy, Stony Brook University, SUNY, Stony Brook, NY 11794, USA
[45]SUBATECH (Ecole des Mines de Nantes, CNRS-IN2P3, Université de Nantes) BP 20722 - 44307, Nantes, France
[46]University of Tennessee, Knoxville, TN 37996, USA
[47]Department of Physics, Tokyo Institute of Technology, Tokyo, 152-8551, Japan
[48]Institute of Physics, University of Tsukuba, Tsukuba, Ibaraki 305, Japan
[49]Vanderbilt University, Nashville, TN 37235, USA
[50]Waseda University, Advanced Research Institute for Science and Engineering, 17 Kikui-cho, Shinjuku-ku, Tokyo 162-0044, Japan
[51]Weizmann Institute, Rehovot 76100, Israel
[52]Yonsei University, IPAP, Seoul 120-749, Korea

(Dated: February 4, 2008)

The invariant differential cross section for inclusive electron production in $p + p$ collisions at $\sqrt{s} = 200$ GeV has been measured by the PHENIX experiment at the Relativistic Heavy Ion Collider over the transverse momentum range $0.4 \leq p_T \leq 5.0$ GeV/c at midrapidity ($|\eta| \leq 0.35$). The contribution to the inclusive electron spectrum from semileptonic decays of hadrons carrying heavy flavor, *i.e.* charm quarks or, at high p_T, bottom quarks, is determined via three independent methods. The resulting electron spectrum from heavy flavor decays is compared to recent leading and next-to-leading order perturbative QCD calculations. The total cross section of charm quark-antiquark pair production is determined as $\sigma_{c\bar{c}} = 0.92 \pm 0.15(\text{stat.}) \pm 0.54(\text{sys.})$ mb.

PACS numbers: 13.85.Qk, 13.20.Fc, 13.20.He, 25.75.Dw

The production of hadrons carrying heavy quarks, *i.e.* charm or bottom, serves as a crucial proving ground

for quantum chromodynamics (QCD), the theory of the strong interaction. Because of the large quark masses, charm and bottom production can be treated by perturbative QCD (pQCD) even at small momenta without being significantly affected by additional soft processes [1]. This is in distinct contrast to the production of particles composed solely of light quarks, which can be evaluated perturbatively only for sufficiently large momenta. Consequently, pQCD calculations of heavy quark production are expected to be reliable over the full momentum range experimentally accessible at collider energies.

For bottom production, next-to-leading order (NLO) calculations are in reasonable agreement with data [2]. Charm measurements at $\sqrt{s} = 1.96$ TeV exist for high transverse momentum (p_T) only [3], where the cross section is higher than NLO predictions by $\geq 50\%$. However, these discrepancies are within the substantial experimental and theoretical uncertainties [3]. At the Relativistic Heavy Ion Collider (RHIC), charm data have been shown for $p+p$ and $d+Au$ collisions at $\sqrt{s_{NN}} = 200$ GeV [4, 5] as well as for Au+Au collisions at 130 and 200 GeV [6, 7]. Further measurements are crucial for a better understanding of heavy flavor production at RHIC. In particular, the relevance of higher order processes and other production mechanisms like jet fragmentation is unclear.

We report on the midrapidity production ($|\eta| \leq 0.35$) of inclusive electrons, $(e^+ + e^-)/2$, in $p+p$ collisions at $\sqrt{s} = 200$ GeV measured by the PHENIX experiment [8] at RHIC. Contributions from semileptonic heavy flavor decays are extracted in the electron p_T range $0.4 \leq p_T \leq 5.0$ GeV/c. The resulting invariant differential cross section is an important benchmark for pQCD calculations of heavy quark production. Furthermore, it provides a crucial baseline for measurements in nuclear collisions at RHIC. Since hadronic heavy flavor production is expected to be dominated by initial parton scattering, systematic studies in $p+p$ and $d+Au$ collisions should be sensitive to the nucleon parton distribution functions as well as to nuclear modifications of these such as shadowing [9]. In Au+Au collisions, heavy quarks constitute a unique and, with the data presented here, calibrated probe for the created hot and dense medium. Possible medium effects on heavy flavor probes include energy loss [10, 11], azimuthal asymmetry [12], and quarkonia suppression [13] or enhancement [14, 15].

The data used here were recorded by PHENIX during RHIC Run-2. Beam-beam counters (BBC), positioned at pseudorapidities $3.1 < |\eta| < 3.9$, measured the collision vertex and provided the minimum bias (MB) interaction trigger defined by at least one hit on each side of the vertex. Events containing high p_T electrons were selected by an additional level-1 trigger in coincidence with the MB trigger. This level-1 trigger required a minimum energy deposit of 0.75 GeV in a 2×2 tile of towers in the electromagnetic calorimeter (EMC) [16]. After a vertex cut of $|z_{vtx}| < 20$ cm, an equivalent of 465×10^6 MB events sampled by the EMC trigger was analyzed in addition to the 15×10^6 events recorded with the MB trigger itself.

The PHENIX east arm spectrometer ($|\eta| < 0.35$, $\Delta\phi = \pi/2$) includes a drift chamber and a pad chamber layer for charged particle tracking. Tracks were confirmed by hits in the EMC matching in position with the track projection within 3σ. Electron candidates required at least two associated hits in the ring imaging Čerenkov detector (RICH) in the projected ring area. Random coincidences of hadron tracks and hits in the RICH occured with a probability of $(3.0 \pm 1.5) \times 10^{-4}$. For electrons the energy E deposited in the EMC equals the momentum p. Requiring $|(E-p)/p| < 3\sigma$, a total charged hadron rejection factor of about 10^4 (10^5) was achieved for $p_T = 0.4$ (≥ 2.0) GeV/c. Remaining background (< 1 %) was measured via event mixing and subtracted statistically.

The differential cross section for electron production was calculated as

$$E\frac{d^3\sigma}{dp^3} = \frac{1}{\epsilon_{bias} \int \mathcal{L}dt} \frac{N_e}{2\pi p_T \Delta y \Delta p_T} \frac{1}{A\epsilon_{rec}}, \qquad (1)$$

where $\int \mathcal{L}dt$ is the integrated luminosity measured with the MB trigger or sampled with the EMC trigger, respectively, ϵ_{bias} is the probability for an electron event to fulfill the MB trigger condition, N_e is the measured electron yield, and $A\epsilon_{rec}$ is the product of geometrical acceptance and reconstruction efficiency. For the EMC triggered sample, ϵ_{rec} includes the trigger efficiency ϵ_{lvl1}.

$\int \mathcal{L}dt$ is calculated as N_{MB}/σ_{BBC}, where N_{MB} is the number of MB triggers or, for the EMC triggered sample, the number of EMC triggers divided by the measured fraction of MB events which simultaneously fulfill the EMC trigger criterion. With the MB trigger cross section $\sigma_{BBC} = 21.8 \pm 2.1$ mb [16], the analyzed data samples correspond to integrated luminosities of 0.7 nb^{-1} (MB trigger) and 21 nb^{-1} (EMC trigger), respectively. The p_T independent trigger bias $\epsilon_{bias} = 0.75 \pm 0.02$ was measured for events containing a π^0 with $p_T > 1.5$ GeV/c [16] and confirmed for charged hadrons with $p_T > 0.2$ GeV/c [17], indicating a universal bias both for hard and soft processes. $A\epsilon_{rec}$ was calculated as a function of p_T (< 10 % variation over the full p_T range) in a GEANT [18] simulation of electrons with flat distributions in rapidity ($|y| < 0.6$), azimuth ($0 < \phi < 2\pi$), and event vertex ($|z| < 30$ cm) as input. The simulated detector response was carefully tuned to match the real detector. Rigorous fiducial cuts were applied to eliminate active area mismatches between data and simulation as well as run-by-run variations. The trigger efficiency ϵ_{lvl1}, evaluated for single electrons in the fiducial area, rises from zero at low p_T to $95 \pm 5\%$ for $p_T > 2$ GeV/c. Finally the effect of finite bin width in p_T was appropriately corrected for.

The corrected electron spectra from the MB and EMC triggered samples cover p_T ranges of $0.4 < p_T < 2.0$ GeV/c and $0.6 < p_T < 5.0$ GeV/c, respectively. They

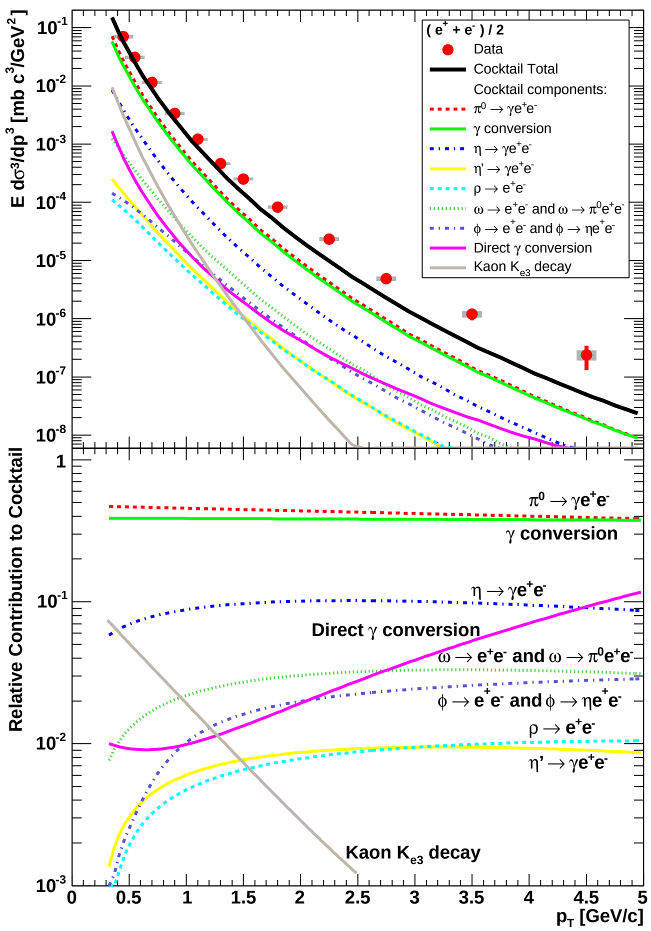

FIG. 1: (Color online) Inclusive electron invariant differential cross section, measured in $p+p$ collisions at $\sqrt{s} = 200$ GeV, compared with all contributions from electron sources included in the background *cocktail* (upper panel). Error bars (boxes) correspond to statistical (systematic) uncertainties. Relative contributions of all electron sources to the background *cocktail* (lower panel).

are consistent with each other within the statistical uncertainties in the p_T region of overlap. The weighted average of both measurements is shown in Fig. 1.

The systematic uncertainty of the inclusive electron spectrum is about 12%, almost p_T independent, calculated as the sum in quadrature of contributions from the acceptance calculation (7%), electron identification cuts (5.2%), run-by-run variations (4%), tracking efficiency (3%), momentum scale (1 - 5%), and other smaller uncertainties. The value of 12% does not include the 9.6% uncertainty of the absolute normalization.

The invariant cross section of electrons from heavy flavor decays was determined by subtracting a *cocktail* of contributions from other sources from the inclusive data. The most important background is the π^0 Dalitz decay which was calculated with a hadron decay generator using a parameterization of measured π^0 [16] and $\pi^{\pm}$ [19]

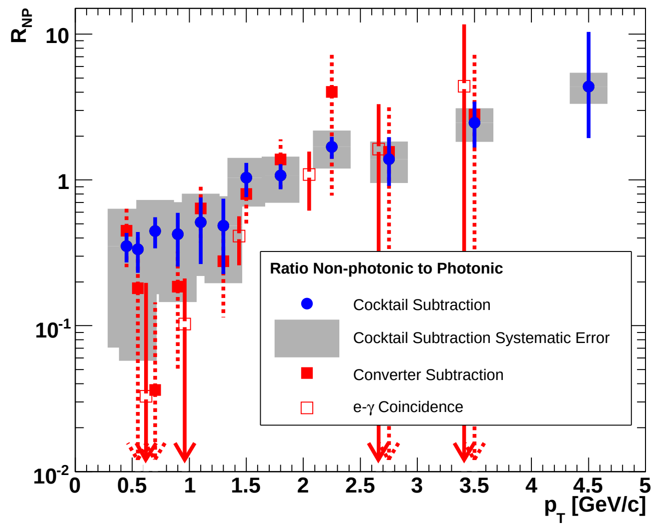

FIG. 2: Ratio of electrons from heavy flavor decays (non-photonic) and other sources (photonic) , R_{NP}, for three independent analysis methods. Error bars (boxes) are statistical (*cocktail* systematic) uncertainties.

spectra as input. The spectral shapes of other light hadrons h were obtained from the pion spectra by m_T scaling. Within this approach the ratios h/π^0 are constant at high p_T and for the relative normalization we used: $\eta/\pi^0 = 0.45 \pm 0.10$ [20], $\rho/\pi^0 = 1.0 \pm 0.3$, $\omega/\pi^0 = 1.0 \pm 0.3$, $\eta'/\pi^0 = 0.25 \pm 0.08$, and $\phi/\pi^0 = 0.40 \pm 0.12$. Only the η contribution is of any practical relevance. Another major electron source is the conversion of photons, mainly from $\pi^0 \to \gamma\gamma$ decays, in material in the acceptance. The spectra of electrons from conversions and Dalitz decays are very similar. In a GEANT simulation of π^0 decays, the ratio of electrons from conversions to electrons from Dalitz decays was determined as 0.73 ± 0.07, essentially p_T independent. Contributions from photon conversions from other sources were taken into account as well. In addition, electrons from kaon decays (K_{e3}), determined in a GEANT simulation based on measured kaon spectra [19], and electrons from external as well as internal conversions of direct photons [21, 22] were considered in the cocktail. All background sources are compared with the inclusive data in the upper panel of Fig. 1 with the relative contributions shown in the lower panel. The total systematic uncertainty of the cocktail is about 12%, essentially p_T independent. This uncertainty is dominated by the systematic error of the pion parameterization ($\approx 10\%$). Other systematic uncertainties, mainly the η/π^0 normalization and, at high p_T, the contribution from direct radiation, are much smaller.

Given the small amount of material in the acceptance (Be beam pipe: 0.29 % X_0; air: 0.28 % X_0) the ratio R_{NP} of non-photonic electrons from heavy flavor decays to background from photonic sources is large ($R_{NP} > 1$ for $p_T > 1.5$ GeV/c) as shown in Fig. 2. Two comple-

mentary analysis methods confirm the *cocktail* result:

The *converter* technique [7] compares electron spectra measured with an additional photon converter $X_C = 1.67\ \%\ X_0$ introduced into the acceptance to measurements without converter. The converter increases the contribution from conversions and Dalitz decays by a fixed factor, which was determined precisely via GEANT simulations. Thus, the electron spectra from photonic and non-photonic sources can be deduced (Fig. 2). The drawbacks of the *converter* method are the limitation in statistics of the converter run period and the fact that the photonic contribution is small at high p_T.

The $e\gamma$ *coincidence* technique evaluates the correlation of electrons and photons via their invariant mass. Electrons from π^0 Dalitz decays or the conversion of one of the photons from $\pi^0 \to \gamma\gamma$ decays are correlated with a photon, in contrast to electrons from semileptonic heavy flavor decays. Comparing the measured $e\gamma$ coincidence rate with the simulated rate for single π^0 events, allows to deduce R_{NP} as shown in Fig. 2, once corrections for contributions from other photonic sources are applied.

After subtracting the background cocktail from the inclusive electron spectrum the invariant differential cross section of electrons from heavy flavor decays is shown in Fig. 3 compared with two theoretical predictions. A leading order (LO) PYTHIA calculation, tuned to existing charm and bottom hadroproduction measurements [23], is in reasonable agreement with the data for $p_T < 1.5$ GeV/c, but underestimates the cross section at higher p_T. It is important to note that this calculation includes a scale factor $K = 3.5$ to accomodate for neglected NLO contributions. A *Fixed-Order plus Next-to-Leading-Log* (FONLL) pQCD calculation [25] still leaves room for further contributions beyond the included NLO processes. The predicted contribution from bottom decays is irrelevant for the electron cross section at $p_T < 3$ GeV/c and becomes significant only for $p_T > 4$ GeV/c.

The charm production cross section was derived from the integrated electron cross section for $p_T > p_{T,low} = 0.6(0.8)$ GeV/c ($d\sigma_e^{p_{T,low}}/dy = 4.78(2.15) \pm 0.78(0.46)(\text{stat.}) \pm 1.74(0.68)(\text{sys.}) \times 10^{-3}$ mb). Since in the low p_T region, which dominates the total cross section, PYTHIA describes the measured spectrum reasonably well, the total charm cross section was determined by extrapolating the properly scaled PYTHIA spectrum to $p_T = 0$ GeV/c. First the PYTHIA spectra for electrons from charm and bottom decays were fit to the data for $p_T > 0.6$ GeV/c, with only the normalizations as free parameters. The resulting midrapidity charm production cross section was determined as $d\sigma_{c\bar{c}}/dy = 0.20 \pm 0.03(\text{stat.}) \pm 0.11(\text{sys.})$ mb, where the systematic error is dominated by the uncertainty of the electron spectrum itself (≈56%), evaluated by refitting PYTHIA to the data at the minimum and maximum of the 1σ systematic error band. Additional uncertainties from the relative ratios of different charmed hadron species and their

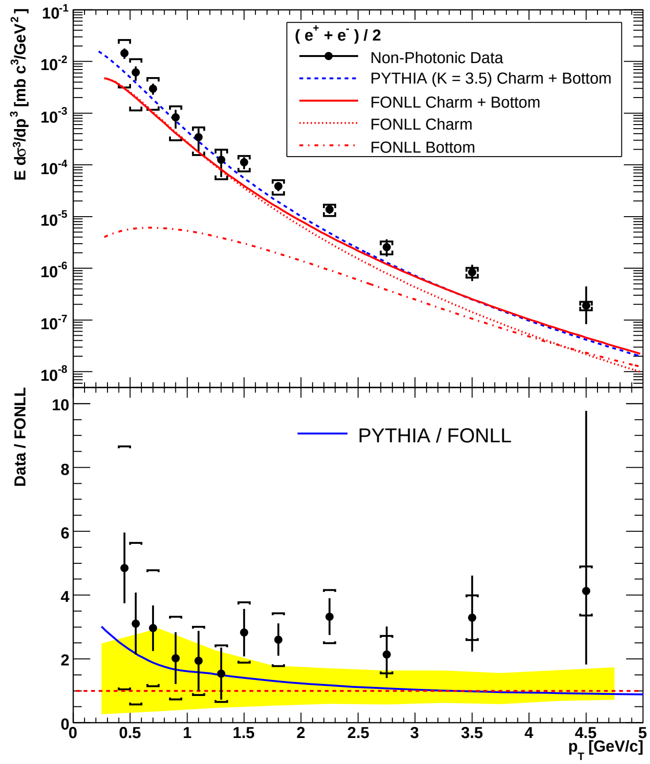

FIG. 3: Invariant differential cross section of electrons from heavy flavor decays compared with PYTHIA LO (with $K = 3.5$) and FONLL pQCD calculations (upper panel). Error bars (brackets) show statistical (systematic) uncertainties. For the FONLL calculation contributions from charm and bottom decays are shown separately. Ratio of data and FONLL calculation (lower panel) with experimental statistical (error bars) and systematic (brackets) uncertainties as well as the theoretical uncertainty (grey band). The solid line corresponds to the ratio of PYTHIA and FONLL.

branching ratios into electrons (≈9%) and the variation of the PYTHIA spectral shape (≈11%) [7] were added in quadrature. The rapidity integrated cross section was determined as $\sigma_{c\bar{c}} = 0.92 \pm 0.15(\text{stat.}) \pm 0.54(\text{sys.})$ mb, where various parton distribution functions (GRV98LO and MRST(c-g) [26] in addition to the default CTEQ5L [24]) were used for the extrapolation, with an associated extra systematic error of ≈6% [7] added in quadrature.

Within errors the integrated charm cross section is compatible with data from $Au + Au$ collisions [7] (minimum bias value: $0.622 \pm 0.057 \pm 0.160$ mb per NN collision) and from $d+Au$ collisions [4] ($1.3 \pm 0.2 \pm 0.4$ mb) at the same $\sqrt{s_{NN}} = 200$ GeV. The FONLL cross section is smaller ($\sigma_{c\bar{c}}^{FONLL} = 0.256^{+0.400}_{-0.146}$ mb) but it is still compatible with the data. Our measurement does not allow to deduce a bottom cross section, which is predicted by FONLL as $\sigma_{b\bar{b}}^{FONLL} = 1.87^{+0.99}_{-0.67}$ μb.

In conclusion, we have measured single electrons from heavy flavor decays in $p + p$ collisions at $\sqrt{s} = 200$ GeV. These data provide a crucial benchmark for pQCD heavy

quark calculations. We observe that above $p_T \approx 2$ GeV/c the electron spectrum is significantly harder than predicted by a LO PYTHIA charm and bottom calculation. Contributions to the charm production cross section in excess of the considered FONLL calculation, *e.g.* from jet fragmentation, can not be excluded. The new data reported here provide an important baseline for the study of medium effects on heavy quark production at RHIC.

We thank the staff of the Collider-Accelerator and Physics Departments at BNL for their vital contributions. We acknowledge support from the Department of Energy and NSF (U.S.A.), MEXT and JSPS (Japan), CNPq and FAPESP (Brazil), NSFC (China), CNRS-IN2P3 and CEA (France), BMBF, DAAD, and AvH (Germany), OTKA (Hungary), DAE and DST (India), ISF (Israel), KRF and CHEP (Korea), RMIST, RAS, and RMAE (Russia), VR and KAW (Sweden), U.S. CRDF for the FSU, US-Hungarian NSF-OTKA-MTA, and US-Israel BSF.

---

* Deceased
† PHENIX Spokesperson:zajc@nevis.columbia.edu

[1] M.L. Mangano *et al.* , Nucl. Phys. **B405**, 507 (1993).
[2] M. Cacciari, hep-ph/0407187; M.L. Mangano, hep-ph/0411020.
[3] D. Acosta *et al.* , Phys. Rev. Lett. **91**, 241804 (2003).
[4] J. Adams *et al.* , Phys. Rev. Lett. **94** 062301 (2005).
[5] S. Kelly *et al.* , J. Phys **G30**, S1189 (2004).
[6] K. Adcox *et al.* , Phys. Rev. Lett. **88**, 192303 (2002).
[7] S.S. Adler *et al.* , Phys. Rev. Lett. **94**, 082301 (2005).
[8] K. Adcox *et al.* , Nucl. Instrum. Methods **A499**, 469 (2003).
[9] Z. Lin and M. Gyulassy, Phys. Rev. Lett. **77**, 1222 (1996).
[10] Y.L. Dokshitzer and D.E. Kharzeev, Phys. Lett. B**519**, 199 (2001).
[11] N. Armesto, A. Dainese, C.A. Salgado, and U.A. Wiedemann Phys. Rev. D**71**, 054027 (2005).
[12] Z.W. Lin and D. Molnar, Phys. Rev. C**68**, 044901 (2003); V. Greco, C.M. Ko, and R. Rapp, Phys. Lett. B**595**, 202 (2004).
[13] T. Matsui and H. Satz, Phys. Lett. B**178**, 416 (1986).
[14] P. Braun-Munzinger and J. Stachel, Phys. Lett. B**490**, 196 (2000).
[15] R.L. Thews, M. Schroedter, and J. Rafelski, Phys. Rev. C**63**, 054905 (2001).
[16] S.S. Adler *et al.* , Phys. Rev. Lett. **91**, 241803 (2003).
[17] S.S. Adler *et al.* , submitted for publication in Phys. Rev. Lett. , hep-ex/0507073.
[18] GEANT 3.21, CERN program library.
[19] F. Matathias *et al.* , J. Phys **G30**, S1113 (2004).
[20] S.S. Adler *et al.* , in preparation.
[21] L.E. Gordon and W. Vogelsang, Phys. Rev. D**50**, 1901 (1994).
[22] S.S. Adler *et al.* , Phys. Rev. D**71**, 071102(R) (2005).
[23] We used PYTHIA 6.205 with a modified set of parameters [6] and CTEQ5L parton distribution functions [24].
[24] H.H. Lai *et al.* , Eur. Phys. J. **C 12**, 375 (2000).
[25] M. Cacciari, P. Nason, and R. Vogt, hep-ph/0502203.
[26] M. Glück, E. Reya, and A. Vogt, Eur. Phys. J. **C 5**, 461 (1998); A.D. Martin, R.G Roberts, W.J. Stirling, and R.S. Thorne, Eur. Phys. J. **C 4**, 463 (1998).